sPHENIX: Experiment overview

Christof Roland[1,*] for the sPHENIX Collaboration
[1]MIT

Abstract. sPHENIX is a newly built state-of-the-art detector at RHIC designed for precision studies of the Quark Gluon Plasma and Cold QCD. It has exceptional reconstruction performance for high-p_T jets, photons and heavy flavor probes with a broad kinematic reach and high rate capability to take large statistics datasets of A+A, p+p and p+A collisions. sPHENIX construction was completed in April 2023. It was commissioned and took first data in the RHIC 2023 Au+Au Run. This paper presents details of the detector design and first physics data from the 2024 p+p and Au+Au runs.

1 Introduction

The sPHENIX experiment [1] at the Relativistic Heavy Ion Collider (RHIC) [2] aims to advance high-energy nuclear physics through the study of high p_{T} and heavy flavor probes. The detector is designed for high rate capability to take large statistics datasets of A+A, p+p and p+A collisions. RHIC and sPHENIX are crucial for exploring the properties of strongly interacting matter and the dynamics of quark-gluon plasma (QGP).

2 The sPHENIX detector

The sPHENIX detector consists of a precision tracking system which enables measurements of heavy-flavor and jet substructure observables, complemented with an electromagnetic and hadronic calorimeter system for measuring the energy of jets and identifying direct photons and electrons.

Going outwards starting from the beam line, sPHENIX comprises the following subsystems [3]: the MAPS-based Vertex Detector (MVTX); the INTermediate Tracker (INTT); the Time Projection Chamber (TPC) [4]; the Time Projection Chamber Outer Tracker (TPOT) [5]; the Electromagnetic Calorimeter (EMCAL) [6, 7]; the Inner Hadronic Calorimeter (IHCAL) [7]; the 1.4 T superconducting solenoid magnet [8] and the Outer Hadronic Calorimeter (OHCAL) [7]. Except for TPOT, all detectors have full azimuthal coverage and span $|\eta| < 1.1$ in pseudorapidity. sPHENIX also includes a number of forward detectors, namely the Minimum Bias Detectors (MBD) which previously served as the PHENIX Beam-Beam Counters [9, 10], the sPHENIX Event Plane Detectors (sEPD), and the Zero Degree Calorimeters (ZDC) which include the Shower Maximum Detector (SMD). The sPHENIX trigger and DAQ system together with the streaming readout capability of the tracking system enable sampling a high interaction rate, especially in p+p collisions, which is crucial for heavy flavor studies.

*e-mail: cer@mit.edu

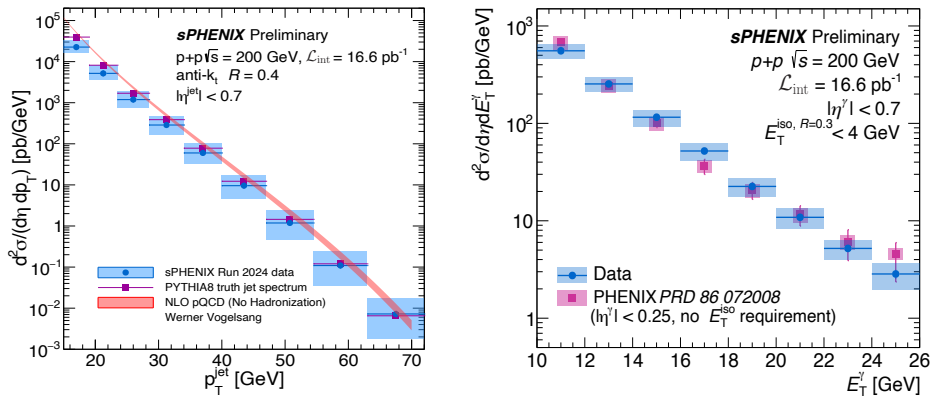

Figure 1. Left: Unfolded jet cross-section for anti-k_t R= 0.4 jets (blue circles), NLO pQCD calculation (red band), and a Pythia-8 Detroit-tune truth jet spectrum (purple squares). Right: The differential cross-section of isolated prompt photons as a function of E_{T}^{γ} is compared with the PHENIX measurements [11] of direct photons. In both panels the blue, vertical bars and shaded boxes represent the statistical and systematic uncertainties, respectively.

sPHENIX began its commissioning process in RHIC Run-2023 with Au+Au collisions at $\sqrt{s_{NN}}$ = 200 GeV. During RHIC Run-2024, sPHENIX collected a large sample of polarized p+p physics data along with a smaller sample of Au+Au data to complete its commissioning phase in that collision system. sPHENIX is actively taking a large Au+Au dataset in 2025, with the goal of collecting 7.2 nb^{-1} of minimum bias data.

3 Detector performance in p+p

Based on the p+p and Au+Au datasets recorded recorded in 2024 the newly built sPHENIX experiment enters the phase of commissioning the physics object reconstruction of the key elements of its science mission. In this report first results on hard probes such as jets and isolated photons are presented as well as first signals of heavy flavor decays.

Jets are reconstructed using the anti-k_t algorithm with radius parameter R = 0.4 using towers in the sPHENIX the electromagnetic, inner, and outer hadronic calorimeters. A jet energy scale calibration is applied to the reconstructed jets and the resulting jet spectrum is unfolded to final state MC particle level [12] based on Pythia-8 [13] simulations of $\sqrt{s}$ = 200 GeV p+p collisions with the Detroit tune propagated through a full Geant4 [14] simulation of the sPHENIX detector. The left panel of Fig. 1 shows the unfolded jet cross-section in p+p collisions at $\sqrt{s}$ = 200 GeV for an integrated luminosity of 16.6 pb^{-1}, or about 15% of the total recorded data set. Overlayed on the figure is a NLO pQCD calculation [15] as well as the Pythia-8 truth jet spectrum. The predictions agree well with the reconstructed jet cross section and already the subset of the available data provides unprecedented statistical reach at RHIC. Based on the reconstructed jet sample, dijets can be reconstructed to study the dijet momentum imbalance $x_J \equiv p_{T,2}/p_{T,1}$ and the dijet angular correlation $\Delta\phi = \phi_1 - \phi_2$with the subscripts 1 and 2 denoting the leading and subleading jet of the dijet [17]. Both the momentum imbalance and the angular correlation of dijets in p+p collisions are important references to study parton energy loss in nuclear collisions at the same collision energy. Figure 2 shows

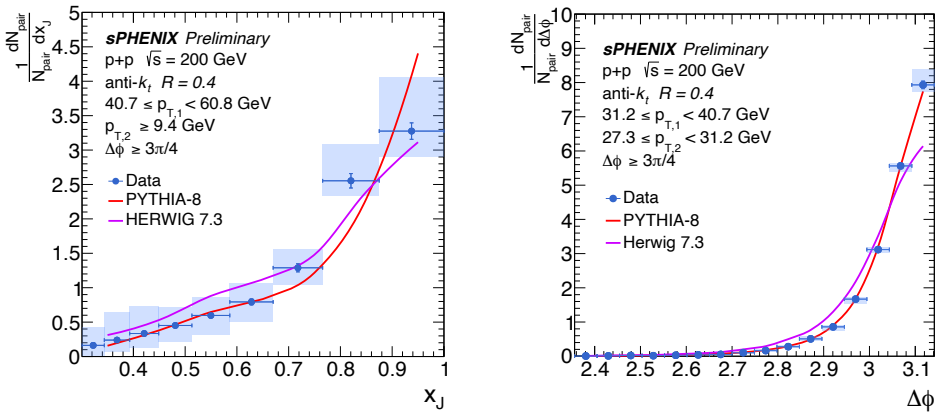

Figure 2. Left: Fully unfolded dijet x_J distribution. Statistical uncertainties are shown as vertical lines and systematic uncertainties as filled boxes. PYTHIA-8 and HERWIG 7.3 generator results are also shown. Right: Dijet $\Delta\phi$ distributions. Statistical uncertainties are shown as vertical lines and systematic uncertainties as filled boxes. PYTHIA-8 and HERWIG 7.3 generator results are also shown.

the $x_J$and $\Delta\phi$ distributions for reconstructed dijets with a leading jet selection of $40.7 \leq p_{T,1} < 60.2$ GeV and a subleading jet of $p_{T,2} > 9.4$ GeV that is opposite the leading jet ($\Delta\phi > 3\pi/4$). The dijet acoplanarity, $\Delta\phi$, is presented with the same leading jet selections. The results are fully unfolded for detector resolution effects.

Isolated prompt photon cross-sections in p+p collisions provide a crucial baseline for identifying possible modifications of the initial parton distributions in nuclear collisions. Isolated prompt photons also serve as an important tool to tag well-defined parton kinematics in photon jet correlations used to study parton energy loss in a nuclear medium. Photon candidates are reconstructed by clustering signals in the electromagnetic calorimeter. Isolated prompt photons are selected by imposing an isolation criterion based on the full information of electromagnetic and hadronic calorimeters in a radius $\Delta R = 0.3$, excluding the E_{T} of the photon candidate of interest [16]. The right panel of Fig. 1 shows the differential cross-section of isolated prompt photons as a function of E_{T}^{γ} in p+p collisions at $\sqrt{s} = 200$ GeV based on the same integrated luminosity as in the left panel.

Decays of heavy flavor carrying particles are reconstructed based on particle trajectories reconstructed in the sPHENIX tracking system. The high magnetic field provides excellent momentum resolution for the tracking system and thus good mass resolution. The precision vertexing based on the silicon detectors allows for precise selection of daughter particles of short-lived heavy flavor particles. In addition, a specific ionization measurement in the TPC provides particle identification to reduce the combinatorial background. Already with early stage detector alignment and calibrations a reconstructed data sample corresponding to an hour of p+p data taking clear invariant mass peaks for $D^0 \rightarrow K^-\pi^+$ and $\Lambda_c^+ \rightarrow p^{\pm}K^{\mp}\pi^{\pm}$ candidates are visible, illustrating the physics performance of sPHENIX for heavy flavor measurements.

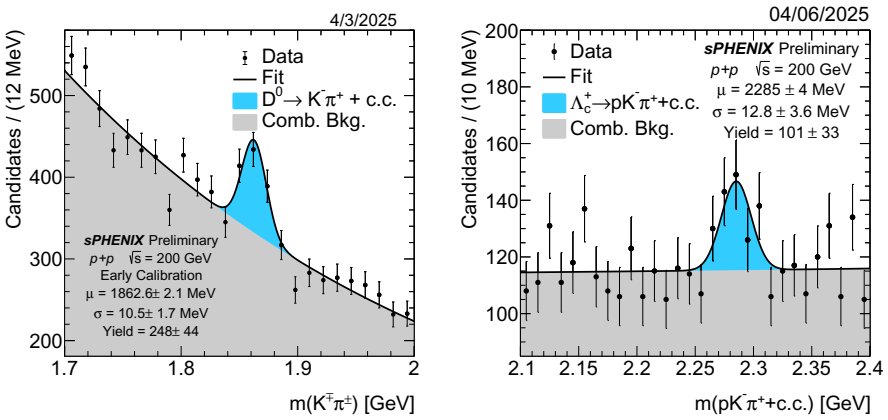

Figure 3. Left: Invariant mass distribution of $K^{\pm}\pi^{\mp}$ pairs. The combinatorial background is shown in gray while the yield of $D^0 \rightarrow K^-\pi^+$ is shown in blue. Right: Invariant mass distribution of $p^{\pm}K^{\mp}\pi^{\pm}$ combinations. The combinatorial background is shown in gray while the yield of $\Lambda_c^+ \rightarrow p^{\pm}K^{\mp}\pi^{\pm}$ is shown in blue.

4 First physics results

As part of its physics commissioning, sPHENIX has remeasured several "standard candles" of heavy ion physics leading to the first physics publications of the collaboration [18, 19].

The charged particle multiplicity $dN_{ch}/d\eta$ produced in nuclear collisions is a fundamental measure of the entropy production of such a collision. Based on the Au+Au dataset recorded in 2024 the charged particle multiplicity is determined by counting tracklets, formed by pairing clusters with a small angular separation from two INTT layers. The analysis approach follows the reconstruction methods employed by the PHOBOS and CMS collaborations [20, 21]. The left panel of Fig. 4 shows $dN_{ch}/d\eta$ at mid-rapidity, averaged over $|\eta| < 0.3$, as a function of the number of participating nucleons of the collision. The reconstructed $dN_{ch}/d\eta$ agrees well with previous measurements [22–25].

Measurements of the transverse energy per unit pseudorapidity, $dE_T/d\eta$, have long been used to estimate the initial energy density reached in nuclear collisions [26]. A sufficiently high energy density is a prerequisite for the formation of a Quark Gluon Plasma. The $dE_T/d\eta$ measurement in sPHENIX is, for the first time at RHIC, based on the energy sums of the calibrated electromagnetic and hadronic calorimeters. The energy sums are corrected for the detector response based on a GEANT4 simulation of the sPHENIX detector. The right panel of Fig. 4 shows $dE_T/d\eta$ as a function of the number of nucleons participating in the collision. The sPHENIX measurement is compatible with previous measurements from PHENIX and STAR [23, 24]

5 Summary

The newly built state-of-the-art sPHENIX detector at RHIC is operational, commissioned, and successfully taking data. sPHENIX is a large-acceptance, high-rate detector that has been optimized for the study of high p_T probes of the quark gluon plasma (QGP) in heavy ion collisions. The primary goal of the experiment is to probe the QGP at shorter length scales by measuring jet and heavy flavor observables that are directly comparable to those at

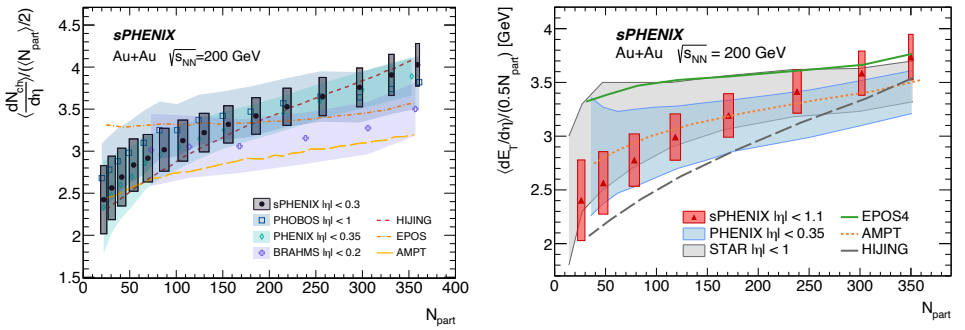

Figure 4. Left: sPHENIX $dN_{ch}/d\eta$ per participant pairs ($N_{part}/2$) at mid-rapidity, as a function of the number of participating nucleons (N_{part}). The sPHENIX results are shown as black solid circles with transparent filled band/boxes indicating total uncertainties. Data from PHOBOS [22], PHENIX [23] and BRAHMS [25] are presented for comparison . The colored bands represent the total systematic uncertainty for each presented measurement. Right: Measured $dE_T/d\eta$ per participant pair, as a function of N_{part}, using the full calorimeter system (red triangles). The vertical size of the boxes indicates the total uncertainty, which includes the uncertainty in N_{part}. Measurements by PHENIX [23] and STAR [24] are shown for comparison, with the vertical size of the band indicating the uncertainty range. MC event generator predictions are shown for EPOS4, AMPT, and HIJING.

the Large Hadron Collider at CERN. First results on fully reconstruced jets, isolated photons and heavy flavor observables from p+p collisions at 200 GeV impressively demonstrate the capablity of sPHENIX to raise the RHIC heavy ion physics program to a new level and to complete its science mission.

References

[1] Adare, A. et al. An Upgrade Proposal from the PHENIX Collaboration. (2015)

[2] Harrison, M., Ludlam, T. & Ozaki, S. RHIC project overview. *Nucl. Instrum. Meth. A*. **499**, 235-244 (2003)

[3] The sPHENIX Collaboration sPHENIX Technical Design Report, PD-2/3 Release. (2019), https://indico.bnl.gov/event/7081/attachments/25527/

[4] Klest, H. Overview and design of the sPHENIX TPC. *J. Phys. Conf. Ser.*. **1498** pp. 012025 (2020)

[5] Aune, S. et al. The sPHENIX Micromegas Outer Tracker. *Nucl. Instrum. Meth. A*. **1066** pp. 169615 (2024)

[6] Aidala, C. et al. Design and Beam Test Results for the 2-D Projective sPHENIX Electromagnetic Calorimeter Prototype. *IEEE Trans. Nucl. Sci.*. **68**, 173-181 (2021)

[7] Aidala, C. et al. Design and Beam Test Results for the sPHENIX Electromagnetic and Hadronic Calorimeter Prototypes. *IEEE Trans. Nucl. Sci.*. **65**, 2901-2919 (2018)

[8] O'Connor, T. et al. Design and testing of the 1.5 T superconducting solenoid for the BaBar detector at PEP-II in SLAC. *IEEE Trans. Appl. Supercond.*. **9** pp. 847-851 (1999)

[9] Ikematsu, K. et al. A Start - timing detector for the collider experiment PHENIX at RHIC-BNL. *Nucl. Instrum. Meth. A*. **411** pp. 238-248 (1998)

[10] Allen, M. et al. PHENIX inner detectors. *Nucl. Instrum. Meth. A*. **499** pp. 549-559 (2003)

[11] Adare, A. et al. Direct photon production in p+p collisions at $\sqrt{s}$ = 200 GeV at midrapidity. *Phys. Rev. D*. **86**, 072008 (2012,10), https://link.aps.org/doi/10.1103/PhysRevD.86.072008

[12] sPHENIX Collaboration, Measurement of the inclusive jet cross-section in p+p collisions at $\sqrt{s}$ = 200 GeV with the sPHENIX detector, sPH-CONF-JET-2025-03.

[13] Sjöstrand, T., Ask, S., Christiansen, J., Corke, R., Desai, N., Ilten, P., Mrenna, S., Prestel, S., Rasmussen, C. & Skands, P. An introduction to PYTHIA 8.2. *Computer Physics Communications*. **191** pp. 159-177 (2015), https://www.sciencedirect.com/science/article/pii/S0010465515000442

[14] S. Agostinelli et al. Geant4—a simulation toolkit. *Nuclear Instruments And Methods In Physics Research Section A: Accelerators, Spectrometers, Detectors And Associated Equipment*. **506**, 250-303 (2003)

[15] Gordon, L. & Vogelsang, W. Polarized and unpolarized prompt photon production beyond the leading order. *Phys. Rev. D*. **48**, 3136-3159 (1993), https://link.aps.org/doi/10.1103/PhysRevD.48.3136

[16] sPHENIX Collaboration, Measurement of isolated photon production in p+p collisions at $\sqrt{s}$ = 200 GeV in sPHENIX, sPH-CONF-JET-2025-02.

[17] sPHENIX Collaboration, Measurement of dijet imbalance (x_J) and acoplanarity ($\Delta\phi$) in p+p collisions at $\sqrt{s}$ = 200 GeV with the sPHENIX detector, sPH-CONF-JET-2025-01.

[18] Abdulhamid, M. et al. Measurement of the transverse energy density in Au+Au collisions at $\sqrt{s_{NN}}$ = 200 GeV with the sPHENIX detector. (2025), https://arxiv.org/abs/2504.02242

[19] Abdulhamid, M. et al. Measurement of charged hadron multiplicity in Au+Au collisions at $\sqrt{s_{NN}}$ = 200 GeV with the sPHENIX detector. (2025), https://arxiv.org/abs/2504.02240

[20] B. Back et al. (PHOBOS Collaboration), Charged-Particle Multiplicity near Midrapidity in Central Au+Au Collisions at $\sqrt{s_{NN}}$ = 56 and 130 GeV. *Phys. Rev. Lett.*. **85** pp. 3100-3104 (2000)

[21] V. Khachatryan et al. (CMS Collaboration), Charged particle multiplicities in pp interactions at $\sqrt{s}$ = 0.9, 2.36, and 7 TeV. *JHEP*. **1** pp. 079 (2011)

[22] B. Alver et al. (PHOBOS Collaboration), Charged-particle multiplicity and pseudorapidity distributions measured with the PHOBOS detector in Au+Au, Cu+Cu d+Au and p+p collisions at ultrarelativistic energies. *Phys. Rev. C*. **83** pp. 024913 (2011)

[23] S.S. Adler et al. (PHENIX Collaboration), Systematic studies of the centrality and $\sqrt{s_{NN}}$ dependence of the $dE_T/d\eta$ and d$N_{\rm ch}$/dη in heavy ion collisions at mid-rapidity. *Phys. Rev. C*. **71** pp. 034908 (2005)

[24] J. Adams et al. Measurements of transverse energy distributions in Au+Au collisions at $\sqrt{s_{NN}}$ = 200 GeV*Phys. Rev. C*. **70**, 054907 (2004,11), https://link.aps.org/doi/10.1103/PhysRevC.70.054907

[25] I.G. Bearden et al. (BRAHMS Collaboration), Pseudorapidity Distributions of Charged Particles from Au+Au Collisions at the Maximum RHIC Energy, $\sqrt{s_{NN}}$ = 200 GeV. *Phys. Rev. Lett.*. **88** pp. 202301 (2002)

[26] J. D. Bjorken, Highly relativistic nucleus-nucleus collisions: The central rapidity region. *Phys. Rev. D*. **27**, 140-151 (1983), https://link.aps.org/doi/10.1103/PhysRevD.27.140